Image charge effects in the nonequilibrium Anderson-Holstein model

E. Perfetto[1] and G. Stefanucci[1,2,3]

[1]*Dipartimento di Fisica, Università di Roma Tor Vergata, Via della Ricerca Scientifica 1, I-00133 Rome, Italy*

[2]*INFN, Laboratori Nazionali di Frascati, Via E. Fermi 40, 00044 Frascati, Italy*

[3]*European Theoretical Spectroscopy Facility (ETSF)*

(Received 25 July 2013; revised manuscript received 6 December 2013; published 23 December 2013)

Image charge effects in nanoscale junctions with strong electron-phonon coupling open the way to unexplored physical scenarios. We propose a simple and still accurate many-body approach to deal with the simultaneous occurrence of the Franck-Condon blockade and the screening-induced enhancement of the polaron mobility. A transparent analytic expression for the polaron decay rate is derived and the dependence on the strength and range of the screening is highlighted. This allows us to interpret and explain several transient and steady-state features of the electrical current. Remarkably, we find that the competition between the charge blocking due to the electron-phonon interaction and the charge deblocking due to the image charges gives rise to a novel mechanism of negative differential conductance. An experimental setup to observe this phenomenon is discussed.

DOI: 10.1103/PhysRevB.88.245437 PACS number(s): 71.38.−k, 73.63.Kv, 81.07.Nb

I. INTRODUCTION

The excitation of quantized vibrational modes due to passage of electrons in a molecular junction is at the origin of a variety of intriguing transport phenomena.[1] In the polaronic (strong coupling) regime electrons are blocked by the Franck-Condon effect and tunneling occurs via excitations of coherent many-phonon states.[2,3] This remarkable charge-transfer process engenders vibrational sidebands in the differential conductance dI/dV, as recently observed in state-of-the-art experiments on carbon nanotube quantum dots (QDs).[4] A proper treatment of Coulomb charging and nuclear trapping already explains several features of the measured dI/dV. Nevertheless, low-dimensional leads screen a charged QD by accumulating holes (image charges[5–10]) in a considerably extended portion nearby the contacts, thus enhancing the electrical current to a large extent (Coulomb deblocking).[11–14] A quantitative assessment of screening effects in polaronic transport is therefore necessary before an exhaustive interpretation of the experimental outcomes can be given.

This paper contains methodological and conceptual advances on the transport properties of screened polarons. We put forward a simple and still accurate method to calculate the relaxation dynamics as well as the steady-state characteristics of biased and/or gated QDs. The key quantity is the polaron decay rate for which we derive a transparent analytic expression, highlighting the impact of the electron-electron (ee) interaction on systems with electron-phonon (ep) coupling. So far numerical simulations have been limited to ep interacting systems and, for all available data, we find excellent agreement.[15–18] In particular the extraordinary long-transient dynamics recently discovered in Ref. 16 is faithfully reproduced. The simultaneous presence of ee and ep interactions opens new scenarios. Relaxation still occurs through a long-lasting sequence of blocking-deblocking events but the distinctive spikes in the transient current become much more pronounced. Noteworthily, the Coulomb deblocking has unexpected repercussions on the steady state. Besides a substantial raising of the phonon-assisted current steps, regions of negative differential conductance (NDC) are found in the dI/dV. The NDC is neither related to the asymmetry of the junction,[19,20] nor to the finite bandwidth of the leads,[21] local charging effects,[3] or range of the tunneling amplitude,[22] and disappears if the ep and ee interactions are considered separately. This novel mechanism, which is of interest on its own, complements the current understanding[19] of NDC observed in QDs.[4]

The paper is organized as follows. In Sec. II we introduce the model Hamiltonian and work out its low-energy expression. Section III contains a detailed presentation of the theoretical framework. We use the bosonization technique and the Lang-Firsov transformation to rewrite the original Hamiltonian in a form suited to deal with the ee and ep interactions nonperturbatively. Then, we derive the equations of motion for the QD Green's function and propose an accurate truncation scheme for their solution. Here we show that polaronic and image charge effects can be incorporated into a correlated embedding self-energy which we calculate analytically. The equations of motion for the Green's function, also known as the Kadanoff-Baym equations, are solved numerically in Sec. IV to extract the transient current. For vanishing ee interactions the accuracy of the approach is demonstrated by comparing the results with exact numerical data.[16] We provide a real-time picture of the Franck-Condon blockade (FCB) and show how the screening changes the FCB scenario. In Sec. V we focus on the steady-state regime. We benchmark the results against available (zero ee interaction) numerically exact I-V characteristics[15] and find good agreement in this case too. In Sec. VI we extend the steady-state analysis and calculate the differential conductance dI/dV as a function of bias and gate voltage. The screening gives rise to regions of NDC similar to those observed in carbon nanotube (CNT) QDs. In Sec. VII we generalize the theory to systems with long-range screening and study the impact of the screening length on the I-V characteristic. The technical details of this generalization are presented in an Appendix. A summary and the main conclusions of this work are drawn in Sec. VIII.

II. LOW-ENERGY HAMILTONIAN

We consider a single-level QD symmetrically connected to two one-dimensional leads of length $\mathcal{L} = \mathcal{N}a$, with a the

lattice spacing and $\mathcal{N}$ the number of lead sites. Electrons on the QD are coupled to a vibrational mode and, at the same time, to electrons in the leads. The Hamiltonian reads

$$\hat{H} = -t_w \sum_{\alpha,j=1}^{\mathcal{N}} (\hat{d}^\dagger_{\alpha j}\hat{d}_{\alpha j+1} + \text{H.c.}) + T_l \sum_{\alpha} (\hat{d}^\dagger_{\alpha 1}\hat{d} + \text{H.c.}) + \epsilon_d \hat{n}_d + \omega_0 \hat{a}^\dagger \hat{a} + \lambda \hat{n}_d (\hat{a}^\dagger + \hat{a}) + U \hat{n}_d \sum_{\alpha} \hat{n}_{\alpha 1}, \quad (1)$$

where the fermion operators $\hat{d}_{\alpha j}$ ($\hat{d}^\dagger_{\alpha j}$) and $\hat{d}$ ($\hat{d}^\dagger$) destroy (create) an electron in the jth site of the $\alpha = L,R$ lead and in the QD, respectively, while the boson operator $\hat{a}$ ($\hat{a}^\dagger$) destroys (creates) the local vibrational quanta.[23] The electron occupation number operators are defined as $\hat{n}_d = \hat{d}^\dagger\hat{d}$ and $\hat{n}_{\alpha j} = \hat{d}^\dagger_{\alpha j}\hat{d}_{\alpha j}$. In Eq. (1) t_w is the (positive) nearest-neighbor hopping in the leads, T_l is the dot-lead tunneling amplitude, ϵ_d is the gate voltage, ω_0 is the phonon frequency, λ is the electron-phonon coupling, and U is the QD-lead Coulomb repulsion. The system is driven out of equilibrium by the sudden switch-on of an external bias $\hat{H}_V = \sum_\alpha V_\alpha \hat{N}_\alpha$, with $\hat{N}_\alpha = \sum_j \hat{n}_{\alpha j}$ the total number of electrons in lead α and $V = V_L - V_R$ the voltage drop. We observe that the Hamiltonian $\hat{H}$ reduces to the interacting resonant level model[12–14,24] for $\lambda = 0$ and to the Anderson-Holstein model[15–17,25–27] for $U = 0$. In a recent work Maier and Komnik studied the nonequilibrium steady-state properties of $\hat{H}$ at the Toulouse point.[28] Here we go beyond their investigation by considering arbitrary couplings U and λ and by extending the analysis to the transient regime.

As we are mainly interested in the small bias behavior, $V \ll t_w$, we derive the low-energy form of Eq. (1) following Ref. 29. In the limit $\mathcal{N} \to \infty$ the Hamiltonian of lead α [first term in Eq. (1)] reads

$$\hat{H}_\alpha = \int_0^{\pi/a} \frac{dk}{2\pi} \epsilon_k \hat{\psi}^\dagger_{\alpha k}\hat{\psi}_{\alpha k}, \quad (2)$$

where $\epsilon_k = -2t_w \cos(ka)$, and the fermion operators

$$\hat{\psi}_{\alpha k} = 2\sqrt{a} \sum_{j=1}^{\infty} \sin(kja)\hat{d}_{\alpha j} \quad (3)$$

satisfy the anticommutation rules $\{\hat{\psi}_{\alpha k}, \hat{\psi}^\dagger_{\alpha' k'}\} = 2\pi\delta_{\alpha\alpha'}\delta(k - k')$. If V is much smaller than the bandwidth $4t_w$ then only electrons with momentum k close to the Fermi momentum $k_F = \pi/(2a)$ contribute to the transport properties. Therefore we linearize the spectrum $\epsilon_k \simeq v_F k$, with $v_F = 2t_w a$ the Fermi velocity, around k_F and extend to $\pm\infty$ the integration limits so that $\hat{H}_\alpha = \int \frac{dk}{2\pi} v_F k\, \hat{\psi}^\dagger_{\alpha k_F+k}\hat{\psi}_{\alpha k_F+k}$. Introducing the field operators $\hat{\psi}_\alpha(x) = \int \frac{dk}{2\pi} e^{ikx}\hat{\psi}_{\alpha k_F+k}$ we find the Dirac Hamiltonian

$$\hat{H}_\alpha = -i v_F \int dx\, \hat{\psi}^\dagger_\alpha(x)\partial_x\hat{\psi}_\alpha(x). \quad (4)$$

In order to complete the low-energy mapping we have to work out the low-energy form of the tunneling and interaction part of $\hat{H}$. This requires one to find a relation between the lattice operator $\hat{d}_{\alpha j}$ and the field operator $\hat{\psi}_\alpha(x)$. We have

$$\hat{d}_{\alpha j} = \sqrt{a}\int_0^{\pi/a} \frac{dk}{\pi}\psi_{\alpha k}\sin(kja) \simeq \sqrt{a}\int_{-\infty}^{\infty} \frac{dk}{\pi}\hat{\psi}_{\alpha k_F+k}\sin[(k_F+k)ja]. \quad (5)$$

For $j = 1$ we can further approximate the right-hand side as

$$\hat{d}_{\alpha 1} \simeq \sqrt{a}\int_{-\infty}^{\infty} \frac{dk}{\pi}\hat{\psi}_{\alpha k_F+k}\sin\left(\frac{\pi}{2} + ka\right) \simeq 2\sqrt{a}\hat{\psi}_\alpha(0). \quad (6)$$

Taking into account that $\hat{n}_{\alpha 1} = \hat{d}^\dagger_{\alpha 1}\hat{d}_{\alpha 1}$ and collecting the pieces together we end up with the low-energy Hamiltonian

$$\hat{H} = -i v_F \sum_\alpha \int_{-\infty}^{\infty} dx\, \hat{\psi}^\dagger_\alpha(x)\partial_x\hat{\psi}_\alpha(x) + \epsilon_d\hat{n}_d + \omega_0\hat{a}^\dagger\hat{a} + t_l\sum_\alpha[\hat{\psi}^\dagger_\alpha(0)\hat{d} + \text{H.c.}] + \lambda\hat{n}_d(\hat{a}^\dagger + \hat{a}) + u\hat{n}_d\sum_\alpha \hat{n}_\alpha(0), \quad (7)$$

where $n_\alpha(x) = \hat{\psi}^\dagger_\alpha(x)\hat{\psi}_\alpha(x)$, $t_l \equiv 2\sqrt{a}T_l$, and $u = 4aU$. In the next section we show how to manipulate Eq. (7) to deal with the ee and ep interactions in a nonperturbative manner.

III. THEORETICAL FRAMEWORK

A. Bosonization and Lang-Firsov transformation

According to the bosonization technique we express the field operators as[30] $\hat{\psi}_\alpha(x) = \frac{\eta_\alpha}{\sqrt{2\pi a}} e^{-2\sqrt{\pi}\, i\hat{\phi}_\alpha(x)}$, with η_α the anticommuting Klein factor and boson field

$$\hat{\phi}_\alpha(x) = i\sum_{q>0}\zeta_q(\hat{b}^\dagger_{\alpha q}e^{-iqx} - \text{H.c.}) - \sqrt{\pi}x\hat{N}_\alpha/\mathcal{L}. \quad (8)$$

In Eq. (8) the quantity $\zeta_q = e^{-aq/2}/\sqrt{2\mathcal{L}q}$ and the operators $\hat{b}^\dagger_{\alpha q} = (2\pi/\mathcal{L}q)^{1/2}\int \frac{dk}{2\pi}\hat{\psi}^\dagger_{\alpha k+q}\hat{\psi}_{\alpha k}$ create particle-hole excitations of momentum q in the leads. Pursuant to the bosonization the lead density reads $\hat{n}_\alpha(x) = \hat{\psi}^\dagger_\alpha(x)\hat{\psi}_\alpha(x) = -\partial_x\hat{\phi}_\alpha(x)/\sqrt{\pi}$, and the Hamiltonian becomes

$$\hat{H} = \sum_{\alpha,q>0} v_F q \hat{b}^\dagger_{\alpha q}\hat{b}_{\alpha q} + \epsilon_d\hat{n}_d + \omega_0\hat{a}^\dagger\hat{a} + t_l\sum_\alpha\left[\frac{\eta^\dagger_\alpha}{\sqrt{2\pi}}e^{-2\sqrt{\pi}\sum_{q>0}\zeta_q(\hat{b}^\dagger_{\alpha q}-\hat{b}_{\alpha q})}\hat{d} + \text{H.c.}\right] + \hat{n}_d\left[\lambda(\hat{a}^\dagger + \hat{a}) - u\sum_{\alpha,q>0}\frac{\zeta_q q}{\sqrt{\pi}}(\hat{b}^\dagger_{\alpha q} + \hat{b}_{\alpha q})\right]. \quad (9)$$

We can now eliminate the ep and ee coupling [third line of Eq. (9)] by performing a Lang-Firsov transformation $\hat{H}' = \hat{\mathcal{U}}^\dagger\hat{H}\hat{\mathcal{U}}$. This is achieved by the unitary operator (from now on sums are over $q > 0$)

$$\hat{\mathcal{U}} = \exp\left[\left(-\frac{\lambda}{\omega_0}(\hat{a}^\dagger - \hat{a}) + \sum_{\alpha q}\frac{u\zeta_q}{\sqrt{\pi}v_F}(\hat{b}^\dagger_{\alpha q} - \hat{b}_{\alpha q})\right)\hat{n}_d\right]. \quad (10)$$

In the explicit form of the transformed Hamiltonian

$$\hat{H}' = \sum_{\alpha q} v_F q \hat{b}^\dagger_{\alpha q}\hat{b}_{\alpha q} + \omega_0 \hat{a}^\dagger\hat{a} + \tilde{\epsilon}_d \hat{n}_d + t_l \sum_\alpha [\hat{f}^\dagger_{\alpha 0}\hat{d} + \text{H.c.}] \tag{11}$$

the QD energy $\tilde{\epsilon}_d = \epsilon_d - \frac{\lambda^2}{\omega_0} - u^2 \sum_q \frac{e^{-aq}}{\pi v_F \mathcal{L}}$ is renormalized by a polaronlike shift and $\hat{f}_{\alpha 0}$ is the screened polaron field

$$\hat{f}_{\alpha x} = \frac{\eta_\alpha}{\sqrt{2\pi a}} e^{-(\lambda/\omega_0)(\hat{a}^\dagger - \hat{a}) + 2\sqrt{\pi}\sum_{\beta q}\zeta_q W_{\alpha\beta}(\hat{b}^\dagger_{\beta q}e^{-iqx} - \hat{b}_{\beta q}e^{iqx})} \tag{12}$$

evaluated in $x = 0$. In this equation $W_{RR} = W_{LL} = 1 - u/(2\pi v_F)$ and $W_{RL} = W_{LR} = -u/(2\pi v_F)$. We emphasize that even though in this work we consider noninteracting leads the derivation above can be generalized to Luttinger liquid leads (for $U = 0$ this has been done in Refs. 31 and 32).

The advantage of working with the bosonized Hamiltonian $\hat{H}'$ is that for $t_l = 0$ the interacting ground state is $|\Psi_{n_d}\rangle = |n_d\rangle \otimes |0_{\text{ph}}\rangle \otimes \prod_{\alpha q} |0_{\alpha q}\rangle$, where $|0_{\text{ph}}\rangle$ and $|0_{\alpha q}\rangle$ are the vacua of the boson operators $\hat{a}$ and $\hat{b}_{\alpha q}$, respectively, and $|n_d\rangle$ is the state of the QD with $n_d = 0$ for $\tilde{\epsilon}_d > 0$ or $n_d = 1$ for $\tilde{\epsilon}_d < 0$. In the following we consider the system initially uncontacted ($t_l = 0$) and then switch on contacts and bias.[33]

B. Equations of motion

Equation (11) is an exact low-energy mapping of the original Hamiltonian. Here we present a simple and accurate truncation scheme to close the equation of motion for the QD Green's function. We define the QD Green's function on the Keldysh contour[35] as $G(z,z') = \frac{1}{i}\langle \mathcal{T}\hat{d}(z)\hat{d}^\dagger(z')\rangle$, where $\mathcal{T}$ is the contour ordering and operators are in the Heisenberg picture with respect to $\hat{H} + \hat{H}_V$ ($\hat{H}_V$ does not change after the Lang-Firsov transformation); the average is taken over $|\Psi_{n_d}\rangle$. The QD Green's function satisfies the equation of motion

$$(i\partial_z - \tilde{\epsilon}_d)G(z,z') = \delta(z,z') + t_l \sum_\alpha G_{\alpha 0}(z,z'), \tag{13}$$

where $G_{\alpha x}(z,z') = \frac{1}{i}\langle \mathcal{T}\hat{f}_{\alpha x}(z)\hat{d}^\dagger(z')\rangle$ is the QD-lead Green's function which in turn satisfies

$$(i\partial_z + i\alpha v_F\partial_x - i\omega_0\lambda\partial_\lambda - V_\alpha)G_{\alpha x}(z,z') = t_l \sum_\beta \frac{1}{i}\langle \mathcal{T}[\hat{f}^\dagger_{\beta 0}\hat{d} + \text{H.c.}, \hat{f}_{\alpha x}](z)\hat{d}^\dagger(z')\rangle. \tag{14}$$

In Eq. (14) we took into account the identity

$$[\omega_0\hat{a}^\dagger\hat{a}, e^{-(\lambda/\omega_0)(\hat{a}^\dagger - \hat{a})}] = \omega_0\lambda\partial_\lambda e^{-(\lambda/\omega_0)(\hat{a}^\dagger - \hat{a})}. \tag{15}$$

The central approximation of our truncation scheme consists in replacing the average on the right-hand side of Eq. (14) with $\langle(\hat{f}^\dagger_{\alpha 0}\hat{f}_{\alpha x} + \hat{f}_{\alpha x}\hat{f}^\dagger_{\alpha 0})(z)\rangle_0 G(z,z')$ where $\langle\cdots\rangle_0$ signifies that operators are in the Heisenberg picture with respect to the uncontacted but biased Hamiltonian. This approximation corresponds to discard virtual tunneling processes between two consecutive ep or ee scatterings and, therefore, becomes exact for $t_l = 0$. Unlike other truncation schemes,[36] however, also the noninteracting case ($\lambda = U = 0$) is *exactly* recovered.

To solve Eq. (14) we define the Green's function $g_{\alpha x\alpha x'}(z,z') = \frac{1}{i}\langle \mathcal{T}\hat{f}_{\alpha x}(z)\hat{f}^\dagger_{\alpha x'}(z')\rangle_0$ with equation of motion

$$(i\partial_z + iv_F\partial_x - i\omega_0\lambda\partial_\lambda - V_\alpha)g_{\alpha x\alpha x'}(z,z') = \delta(z,z')\langle(\hat{f}_{\alpha x}\hat{f}^\dagger_{\alpha x'} + \hat{f}^\dagger_{\alpha x'}\hat{f}_{\alpha x})(z)\rangle_0. \tag{16}$$

Therefore

$$G_{\alpha x}(z,z') = t_l \int d\bar{z}\, g_{\alpha x\alpha 0}(z,\bar{z})G(\bar{z},z') \tag{17}$$

and inserting this result into Eq. (13) we obtain a closed equation for the QD Green's function

$$(i\partial_z - \tilde{\epsilon}_d)G(z,z') - \int d\bar{z} \sum_\alpha \Sigma_\alpha(z,\bar{z})G(\bar{z},z') = \delta(z,z'). \tag{18}$$

In this equation

$$\Sigma_\alpha(z,z') = t_l^2 g_{\alpha 0\alpha 0}(z,z') \tag{19}$$

is a correlated embedding self-energy whose greater/lesser Keldysh components are related to the decay rate for an added/removed polaron. In fact, $\Sigma^>_\alpha(t,t')$ is proportional to the amplitude for an electron in the QD to tunnel in lead α at time t', explore virtually the lead for a time $t - t'$, and tunnel back to the QD at time t. A similar interpretation applies to $\Sigma^<_\alpha$. Using the Langreth rules[35] we convert Eq. (18) into a coupled system of Kadanoff-Baym equations[38–42] which we then solve numerically once an expression for Σ_α is given.

The Green's function $g_{\alpha x\alpha x'}(z,z')$ can be calculated analytically being the average of coherent-state operators over the bosonic vacua. The greater/lesser Keldysh components read

$$g^{\lessgtr}_{\alpha x\alpha x'}(t,t') = \pm\frac{ia^{\beta-1}e^{-g}e^{ge^{\pm i\omega_0(t-t')}}e^{-iV_\alpha(t-t')}}{2\pi[a \mp iv_F(t-t') \pm i(x-x')]^\beta}, \tag{20}$$

with ratio $g = (\lambda/\omega_0)^2$ and u-dependent exponent $\beta = 1 + \frac{u(u-2\pi v_F)}{2\pi^2 v_F^2}$. Inserting this result into Eq. (19) we find

$$\Sigma^{\lessgtr}_\alpha(t-t') = \pm\frac{i\Lambda\Gamma e^{-g}}{2\pi}\frac{e^{ge^{\pm i\omega_0(t-t')}}}{[1 \mp i\Lambda(t-t')]^\beta}e^{-iV_\alpha(t-t')}, \tag{21}$$

where $\Gamma = 2T_l^2/t_w = t_l^2/v_F$ is the level broadening and $\Lambda = v_F/a$ is the high-energy cutoff.

IV. TRANSIENT REGIME

From the solution of Eq. (18) we can extract the time-dependent (TD) QD density as well as the TD current $I_\alpha(t)$ at the α interface

$$I_\alpha(z) = \int d\bar{z}\, \Sigma_\alpha(z,\bar{z})G(\bar{z},z) + \text{H.c.} \tag{22}$$

We apply a symmetric bias $V_L = -V_R = V/2$ and calculate $I(t) = [I_L(t) + I_R(t)]/2$ for the parameters of Fig. 1. The $U = 0$ curve is almost on top of the diagrammatic Monte Carlo simulation.[16] The TD current displays quasistationary plateaus between two consecutive times $2n\pi/\omega_0$; around these times we see sharp spikes. For $U > 0$ we observe a significant enhancement of the current; the plateaus bend and the amplitude of the spikes increases. We understand this peculiar transient behavior by inspecting the self-energy

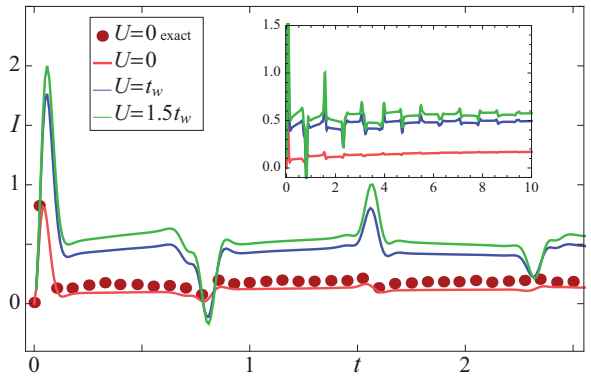

FIG. 1. (Color online) TD current for different U at fixed λ, and initial QD occupancy $n_d = 1$. For $U = 0$, exact data from Ref. 16 are also displayed (circles). The parameters are $\lambda = 16$, $\omega_0 = 8$, $V = 26$, $\tilde{\epsilon}_d = -10$, and $\Lambda = 100$. Units: $10^{-1}\Gamma$ for energies and Γ^{-1} for times. Inset: $I(t)$ for long propagation times (not within reach of current numerical techniques).

in Eq. (21). In the top panel of Fig. 2 we plot $|\Sigma^<(t)|$ for increasing λ at $U = 0$. The effect of the ep interaction is twofold: an overall suppression proportional to e^{-g} and a modulation of period $2\pi/\omega_0$ (coming from the double exponential $e^{e^{i\omega_0 t}}$). Physically (see cartoon in the top panel of Fig. 2), if we start at time $t = T$ with one electron on the QD the phonon cloud is centered around the minimum at $x \simeq \lambda/\omega_0^2$ of the harmonic potential. The large $|\Sigma^<(T)|$ favors the transfer of the electron from the QD to the leads causing a sudden shift of the minimum to $x = 0$. At this point the polaron (electron + cloud) cannot hop back to the QD since

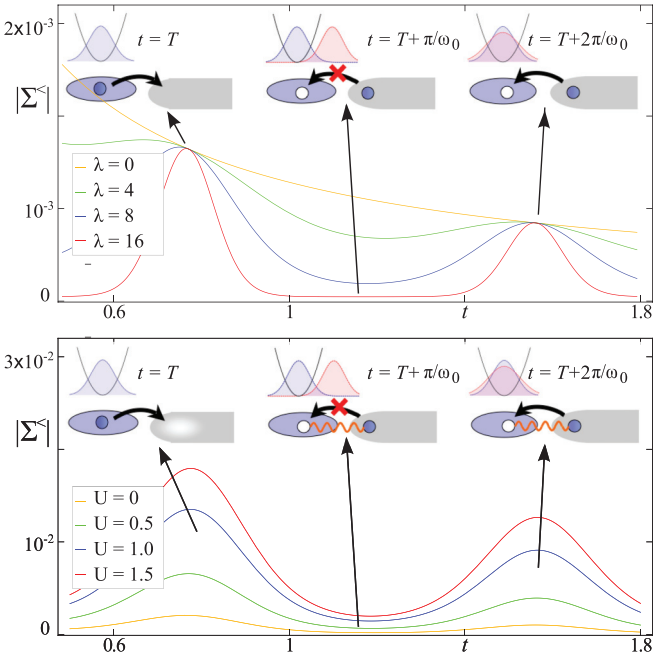

FIG. 2. (Color online) Modulus of the TD self-energy $|\Sigma^<_\alpha(t)|$ for different λ at $U = 0$ (top panel), and for different U (in units of t_w) at $\lambda = 8$ (bottom panel). The parameters are $\omega_0 = 8$, $\tilde{\epsilon}_d = 0$, and $\Lambda = 100$. Units: $\Lambda\Gamma$ for $|\Sigma^<|$, Γ for energies, and Γ^{-1} for times.

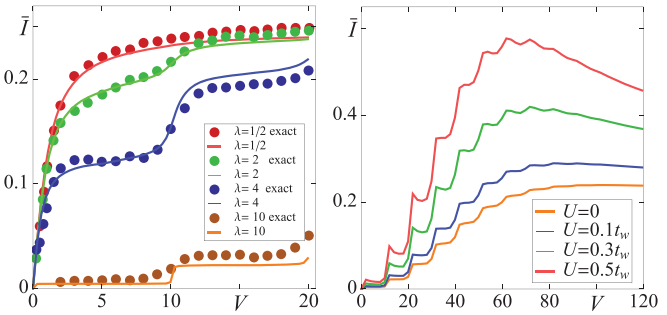

FIG. 3. (Color online) I-V curve for different λ at $U = 0$ (left panel), and for different U at $\lambda = 10$ (right panel). The parameters are $\omega_0 = 5$, $\tilde{\epsilon}_d = 0$, and $\Lambda = 1000$. For $U = 0$ (left panel), exact data from Ref. 15 are also displayed (circles). All energies in units of Γ.

the overlap between the shifted phonon-cloud wave functions is negligible (small $|\Sigma^<(t)|$). Only after a dwelling time of order $2\pi/\omega_0$ this overlap is again sizable, the electron returns to the QD (large $|\Sigma^<(T + 2\pi/\omega_0)|$), and the cycle restarts. The physical interpretation offered by Eq. (21) enables us to explain the structure of the transient, how the system approaches the FCB regime, and how image-charge effects change the picture. Indeed, a nonvanishing U modifies the envelope of $|\Sigma^<|$ from the noninteracting power law $1/t$ to $1/t^\beta$ (see bottom panel of Fig. 2). According to the cartoon an electron in the QD causes a depletion of charge (image-charge effect) in the vicinity of the interface, thus facilitating the tunneling (Coulomb deblocking).[11–14] Similarly, when the electron is in the leads the hole left on the QD acts as an attractive potential and the probability to tunnel back increases. This explains the enhancement of I in Fig. 1.

V. STEADY STATE

In the steady-state regime G and Σ_α depend only on the time difference and can be Fourier transformed. The steady current $\bar{I}$ is given by a Meir-Wingreen-like formula[14,25]

$$\bar{I} = \int \frac{d\omega}{2\pi} \frac{\Sigma_L^>(\omega)\Sigma_R^<(\omega) - \Sigma_L^<(\omega)\Sigma_R^>(\omega)}{\left|\omega - \tilde{\epsilon}_d - \sum_\alpha \Sigma_\alpha^{\mathrm{R}}(\omega)\right|^2}, \qquad (23)$$

where the explicit expression for the self-energy in frequency space reads

$$\Sigma_\alpha^{\lessgtr}(\omega) = \pm i \frac{\Gamma e^{-g}}{\Gamma(\beta)} \sum_{n=0}^{\infty} \frac{g^n}{n!} |\omega_{\alpha n}^{\lessgtr}/\Lambda|^{\beta-1} \theta(\pm\omega_{\alpha n}^{\lessgtr}), \qquad (24)$$

with $\omega_{\alpha n}^{\lessgtr} = \omega \pm n\omega_0 - V_\alpha$, $\Gamma(\beta)$ the Euler-gamma function, and θ the Heaviside step function.[43]

In Fig. 3 we show the I-V curve for different λ at $U = 0$ (left panel), and for different U at fixed $\lambda = 10$ (right panel). The former is benchmarked against real-time path-integral Monte Carlo results.[15] Again we find quantitative agreement from weak to strong coupling. The FCB suppression of $\bar{I}$ at large λ as well as the phonon-assisted current steps at $V = 2\omega_0$ are correctly reproduced. Turning on the ee interaction the Coulomb deblocking takes place and $\bar{I}$ increases for all V. We still observe phonon-assisted steps but, unexpectedly,

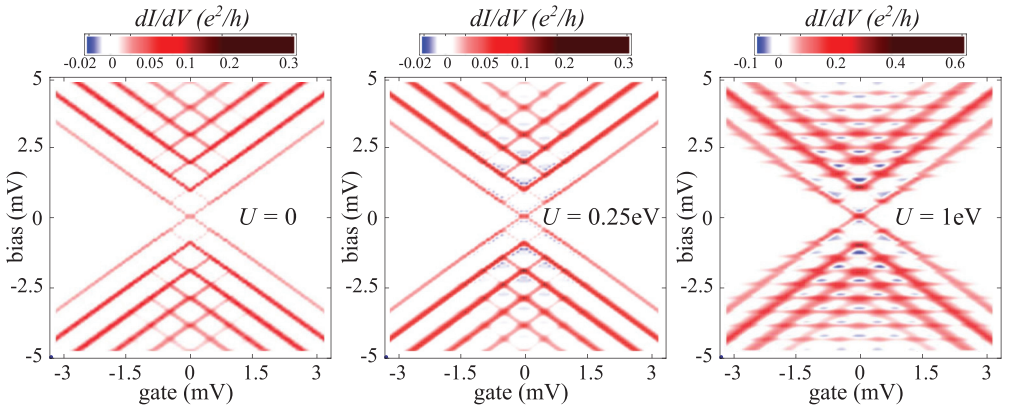

FIG. 4. (Color online) Contour plot of the differential conductance dI/dV as a function of gate $\tilde{\epsilon}_d$ and bias V, for three different dot-lead repulsion: $U = 0$ (left panel), $U = 0.25$ eV (middle panel), and $U = 1$ eV (right panel). The rest of the parameters are specified in the text.

they bend *downward* giving rise to regions of NDC. This phenomenon is driven by the competition between ee and ep interactions (no NDC for $U = 0$ or $\lambda = 0$). By further increasing the bias a crossover occurs: The steps are attenuated and the current acquires a power-law decay $\bar{I} \sim V^{\beta-1}$. In this region the system behaves as if the ep coupling were zero.[14,24]

VI. NEGATIVE DIFFERENTIAL CONDUCTANCE

We investigate further the NDC aspect by calculating the dI/dV as a function of voltage V and gate $\tilde{\epsilon}_d$. NDC regions have been observed in QDs formed between the defects of a CNT.[4] Even though theoretical studies have so far focussed on the ep coupling,[4,19] the left/right portion of the CNT screens the charge accumulated on the QD. Our Hamiltonian represents the simplest generalization of previous models to include this image-charge effect. We use parameters from the literature: $\omega_0 = 1$ meV, $\lambda = 1.82$ meV, $a = 2.46$ Å, $v_F = 8.1 \times 10^5$ m/s, $\Gamma = 0.1$ meV, and $\Lambda = 0.1$ eV.[44] For the ee coupling we take $U < 1$ eV, since in CNTs the on-site repulsion is ~ 5 eV.[45] In Fig. 4 we show the contour plot of the dI/dV for three different Us. The $U = 0$ case accurately reproduces the FCB diamonds obtained within the rate equations approach[3] and later observed in experiments.[4] However, no signatures of NDC are found. For $U = 0.25$ eV, instead, spots of NDC appear inside the diamonds, in qualitative agreement with the experiment. Increasing U even further the NDC regions expand, and horizontal stripes of large conductance emerge. These stripes are suppressed by the strong, local repulsion (not considered here) responsible for the Coulomb blockade.[3]

VII. GENERALIZATION TO LONG-RANGE INTERACTIONS

Our approximation scheme can be generalize to deal with long-range QD-lead ee interactions. We consider an interaction $u(x)$ between an electron in the QD and a density fluctuation $n(x)$ at distance x. The generalization of Eq. (7) is

$$\hat{H} = -iv_F \sum_{\alpha=L,R} \int_{-\infty}^{\infty} dx\, \hat{\psi}^\dagger_\alpha(x)\partial_x\hat{\psi}_\alpha(x) + \epsilon_d\hat{n}_d + \omega_0\hat{a}^\dagger\hat{a} + t_l \sum_\alpha [\hat{\psi}^\dagger_\alpha(0)\hat{d} + \text{H.c.}] + \lambda\hat{n}_d(\hat{a}^\dagger + \hat{a}) + \hat{n}_d \sum_\alpha \int_{-\infty}^{\infty} dx\, u(x)\hat{n}_\alpha(x). \quad (25)$$

The contact interaction previously considered is recovered for $u(x) = u\delta(x)$. The correlated embedding self-energy is still given by Eq. (19) but the Green's function g now reads (see Appendix)

$$g^{\lessgtr}_{\alpha 0\alpha 0}(t,t') = \pm\frac{i}{2\pi a} e^{-g} e^{Q[\pm(t-t')]} e^{ge^{\pm i\omega_0(t-t')}} e^{-iV_\alpha(t-t')}, \quad (26)$$

with exponent

$$Q(t) = \sum_q \frac{2\pi}{\mathcal{L}q} e^{-aq}(e^{iv_F qt} - 1)\left[1 - \frac{u_q}{\pi v_F} + \frac{1}{2}\left(\frac{u_q}{\pi v_F}\right)^2\right]. \quad (27)$$

In Fig. 5 we display the I-V characteristic of the soft-Coulomb interaction $u(x) = u/\sqrt{x^2 + a^2}$ (solid lines) and compare it

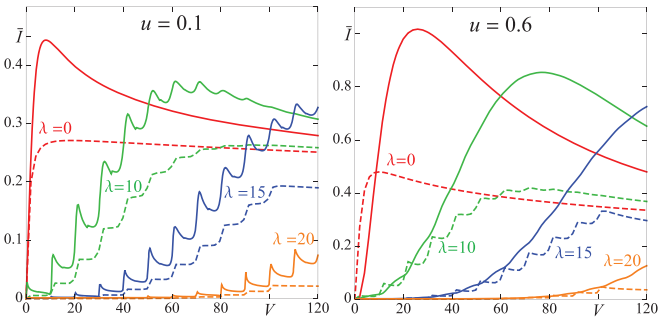

FIG. 5. (Color online) I-V curves for $u(x) = u/\sqrt{x^2 + a^2}$ (solid lines) and $u(x) = u\delta(x)$ (dashed lines) for different values of the ep coupling: $\lambda = 0$ (red), $\lambda = 10$ (green), $\lambda = 15$ (blue), and $\lambda = 20$ (orange). In the left panel $u = 0.1$, and in the right panel $u = 0.6$. The rest of the parameters are $\omega_0 = 5$, $\tilde{\epsilon}_d = 0$, and $\Lambda = 1000$. Energies are in units of $\Gamma/2$ and u is in units of v_F.

with the I-V characteristic of the contact interaction $u(x) = u\delta(x)$ (dashed lines) for $u = 0.1v_F$ (left panel) and $u = 0.6v_F$ (right panel) at different values of λ. The long-range interaction tends to increase the current since the depletion of charge extends over a longer portion of the leads (enhancement of the Coulomb deblocking). The consequences for the NDC are that for small u (left panel) the NDC is more pronounced, while for large u the NDC is significantly suppressed.

VIII. SUMMARY AND CONCLUSIONS

We presented a comprehensive analysis of the nonequilibrium properties of a QD with an ep coupling λ and an ee QD-lead repulsion U. The Hamiltonian reduces to the interacting resonant level model for $\lambda = 0$ and to the Anderson-Holstein model for $U = 0$. Here we considered the presence of arbitrary couplings U and λ. Combining the bosonization method with nonequilibrium Green's function theory we obtained the Kadanoff-Baym equations for the QD Green's function. The self-energy is approximated using a truncation scheme in the polaronic basis and has a simple analytic form which accounts for the level broadening due to the leads as well as for the ep and ee interactions. Excellent agreement with available numerical results is found in the transient and in the steady-state regime. The formula for the self-energy renders the physical interpretation of the results direct and intuitive. We also showed that the competition between FCB and Coulomb deblocking leads to a novel mechanism for the NDC, and studied the dependence on the screening length. This NDC mechanism occurs in QD weakly coupled to low-dimensional leads, like those recently realized with CNT.

ACKNOWLEDGMENTS

We acknowledge funding by MIUR FIRB Grant No. RBFR12SW0J.

APPENDIX : EVALUATION OF Σ FOR LONG-RANGE INTERACTIONS

By introducing the Fourier transform $u_q = \int dx\, e^{iqx}u(x)$ and the bosonized form of the field operators, the Hamiltonian of Eq. (25) becomes

$$\begin{aligned}\hat{H} = &\sum_{\alpha,q>0} v_F q \hat{b}^\dagger_{\alpha q}\hat{b}_{\alpha q} + \epsilon_d \hat{n}_d + \omega_0 \hat{a}^\dagger\hat{a}\\ &+t_l \sum_\alpha \left[\frac{\eta^\dagger_\alpha}{\sqrt{2\pi}} e^{-2\sqrt{\pi}\sum_{q>0}\zeta_q(\hat{b}^\dagger_{\alpha q}-\hat{b}_{\alpha q})}\hat{d} + \text{H.c.}\right]\\ &+\hat{n}_d\left[\lambda(\hat{a}^\dagger+\hat{a}) - \sum_{\alpha,q>0}\frac{\zeta_q q}{\sqrt{\pi}}u_q(\hat{b}^\dagger_{\alpha q}+\hat{b}_{\alpha q})\right],\end{aligned} \tag{A1}$$

where the zero-mode contribution has been discarded as it vanishes for leads of infinite length. As in the short-range case we perform a Lang-Firsov transformation $\hat{H}' = \hat{\mathcal{U}}^\dagger\hat{H}\hat{\mathcal{U}}$ to eliminate the ep and ee coupling [second line of Eq. (A1)]. This is achieved by the unitary operator (sums over $q > 0$ are understood)

$$\hat{\mathcal{U}} = \exp\left[\left(-\frac{\lambda}{\omega_0}(\hat{a}^\dagger-\hat{a}) + \sum_{\alpha q}\frac{\zeta_q}{\sqrt{\pi}v_F}u_q(\hat{b}^\dagger_{\alpha q}-\hat{b}_{\alpha q})\right)\hat{n}_d\right]. \tag{A2}$$

After the Lang-Firsov transformation we end up with a Hamiltonian $\hat{H}'$ which is *formally identical* to the one in Eq. (11) with the only difference that

$$\tilde{\epsilon}_d = \epsilon_d - \frac{\lambda^2}{\omega_0} - \sum_q u_q^2 \frac{e^{-aq}}{\pi v_F \mathcal{L}} \tag{A3}$$

and

$$\hat{f}_{\alpha x} = \frac{\eta_\alpha}{\sqrt{2\pi a}} e^{-(\lambda/\omega_0)(\hat{a}^\dagger-\hat{a})+2\sqrt{\pi}\sum_{\beta q}\zeta_q W_{\alpha\beta q}(\hat{b}^\dagger_{\beta q}e^{-iqx}-\hat{b}_{\beta q}e^{iqx})}, \tag{A4}$$

with

$$\begin{aligned}W_{RRq} &= W_{LLq} = 1 - u_q/(2\pi v_F),\\ W_{RLq} &= W_{LRq} = -u_q/(2\pi v_F).\end{aligned} \tag{A5}$$

The screened polaron field is again a coherent-state operator and therefore the Green's function $g_{\alpha x\alpha' x'}(z,z') = \frac{1}{i}\langle \mathcal{T}\hat{f}_{\alpha x}(z)\hat{f}^\dagger_{\alpha' x'}(z')\rangle_0$ can be calculated analytically using standard identities for the harmonic oscillator. The result is given in Eqs. (26) and (27) and correctly reduces to Eq. (20) in the case of contact interactions $u_q = u$.

[1] M. Galperin, M. A. Ratner, A. Nitzan, and A. Troisi, Science **319**, 1056 (2008).
[2] J. Koch, F. J. von Oppen, and A. V. Andreev, Phys. Rev. B **74**, 205438 (2006).
[3] J. Koch and F. J. von Oppen, Phys. Rev. Lett. **94**, 206804 (2005).
[4] R. Leturcq, C. Stampfer, K. Inderbitzin, L. Durrer, C. Hierold, E. Mariani, F. von Oppen, and K. Ensslin, Nat. Phys. **5**, 327 (2009).
[5] J. B. Neaton, M. S. Hybertsen, and S. G. Louie, Phys. Rev. Lett. **97**, 216405 (2006).
[6] K. S. Thygesen and A. Rubio, Phys. Rev. Lett. **102**, 046802 (2009).
[7] J. M. Garcia-Lastra, C. Rostgaard, A. Rubio, and K. S. Thygesen, Phys. Rev. B **80**, 245427 (2009).
[8] K. Kaasbjerg and K. Flensberg, Nano Lett. **8**, 3809 (2008).
[9] K. Kaasbjerg and K. Flensberg, Phys. Rev. B **84**, 115457 (2011).
[10] P. Myöhänen, R. Tuovinen, T. Korhonen, G. Stefanucci, and R. van Leeuwen, Phys. Rev. B **85**, 075105 (2012).
[11] G. D. Mahan, Phys. Rev. Lett. **18**, 448 (1967); P. Nozières and C. T. De Dominicis, Phys. Rev. **178**, 1097 (1969).
[12] J. Spitaler, E. Ya. Sherman, H. G. Evertz, and C. Ambrosch-Draxl, Phys. Rev. B **70**, 125107 (2004).
[13] M. Goldstein, R. Berkovits, and Y. Gefen, Phys. Rev. Lett. **104**, 226805 (2010).
[14] E. Perfetto, G. Stefanucci, and M. Cini, Phys. Rev. B **85**, 165437 (2012).
[15] L. Mühlbacher and E. Rabani, Phys. Rev. Lett. **100**, 176403 (2008).
[16] K. F. Albrecht, A. Martin-Rodero, R. C. Monreal, L. Mühlbacher, and A. Levy Yeyati, Phys. Rev. B **87**, 085127 (2013).

[17]E. Y. Wilner, H. Wang, G. Cohen, M. Thoss, and E. Rabani, Phys. Rev. B **88**, 045137 (2013).
[18]H. Wang and M. Thoss, J. Chem. Phys. **138**, 134704 (2013).
[19]F. Cavaliere, E. Mariani, R. Leturcq, C. Stampfer, and M. Sassetti, Phys. Rev. B **81**, 201303(R) (2010).
[20]R. Härtle and M. Thoss, Phys. Rev. B **83**, 115414 (2011).
[21]M. Galperin, M. A. Ratner, and A. Nitzan, Nano Lett. **5**, 125 (2005).
[22]A. Zazunov, D. Feinberg, and T. Martin, Phys. Rev. B **73**, 115405 (2006).
[23]T. Holstein, Ann. Phys. (N.Y.) **8**, 325 (1959).
[24]E. Boulat, H. Saleur, and P. Schmitteckert, Phys. Rev. Lett. **101**, 140601 (2008).
[25]N. S. Wingreen, K. W. Jacobsen, and J. W. Wilkins, Phys. Rev. B **40**, 11834 (1989).
[26]A. P. Jauho, N. S. Wingreen, and Y. Meir, Phys. Rev. B. **50**, 5528 (1994).
[27]S. Maier, T. L. Schmidt, and A. Komnik, Phys. Rev. B **83**, 085401 (2011).
[28]S. Maier and A. Komnik, Phys. Rev. B **82**, 165116 (2010).
[29]E. Miranda, Braz. J. Phys. **33**, 3 (2003).
[30]T. Giamarchi, *Quantum Physics in One Dimension* (Clarendon, Oxford, 2004).
[31]G. A. Skorobagatko and I. V. Krive, Low Temp. Phys. **34**, 858 (2008).
[32]G. A. Skorobagatko, Phys. Rev. B **85**, 075310 (2012).
[33]The initial-state dependence due to the contacts is washed out in the long-time limit.[34]
[34]E. Perfetto, G. Stefanucci, and M. Cini, Phys. Rev. Lett. **105**, 156802 (2010).
[35]G. Stefanucci and R. van Leeuwen, *Nonequilibrium Many- Body Theory of Quantum Systems: A Modern Introduction* (Cambridge University Press, Cambridge, UK, 2013).
[36]We briefly discuss the differences with an alternative approach to deal with ep interactions ($U = 0$) (Ref. 37). Our correlator between the f fields is not dressed by virtual tunneling processes, whereas in Ref. 37 this dressing is accounted for up to second order in a self-consistent manner. However, in Ref. 37 the Green's function satisfies Eq. (18) in which the G under the integral sign is replaced by the noninteracting G_0. Consequently the noninteracting case ($\lambda = 0$) is not recovered.
[37]M. Galperin, A. Nitzan, and M. A. Ratner, Phys. Rev. B **73**, 045314 (2006).
[38]N. E. Dahlen and R. van Leeuwen, Phys. Rev. Lett. **98**, 153004 (2007).
[39]P. Myöhänen, A. Stan, G. Stefanucci, and R. van Leeuwen, Europhys. Lett. **84**, 67001 (2008).
[40]P. Myöhänen, A. Stan, G. Stefanucci, and R. van Leeuwen, Phys. Rev. B **80**, 115107 (2009).
[41]M. Puig von Friesen, C. Verdozzi, and C.-O. Almbladh, Phys. Rev. Lett. **103**, 176404 (2009).
[42]M. Puig von Friesen, C. Verdozzi, and C.-O. Almbladh, Phys. Rev. B **82**, 155108 (2010).
[43]The retarded component of Σ_α in Eq. (23) is extracted from $\Sigma^{\mathrm{R}}_\alpha(\omega) = \int \frac{d\omega'}{2\pi i} \frac{\Sigma^<_\alpha(\omega') - \Sigma^>_\alpha(\omega')}{\omega - \omega' + i\eta}$.
[44]J. González and E. Perfetto, Phys. Rev. B **72**, 205406 (2005); E. Perfetto and J. González, *ibid.* **74**, 201403 (2006).
[45]E. Perfetto, M. Cini, S. Ugenti, P. Castrucci, M. Scarselli, M. De Crescenzi, F. Rosei, and M. A. El Khakani, Phys. Rev. B **76**, 233408 (2007).